

The nonlinear electromigration of analytes into confined spaces

BY ZHEN CHEN AND SANDIP GHOSAL*

*Department of Mechanical Engineering, Northwestern University,
2145 Sheridan Road, Evanston, IL 60208, USA*

We consider the problem of electromigration of a sample ion (analyte) within a uniform background electrolyte when the confining channel undergoes a sudden contraction. One example of such a situation arises in microfluidics in the electrokinetic injection of the analyte into a micro-capillary from a reservoir of much larger size. Here, the sample concentration propagates as a wave driven by the electric field. The dynamics is governed by the Nernst–Planck–Poisson system of equations for ionic transport. A reduced one-dimensional nonlinear equation, describing the evolution of the sample concentration, is derived. We integrate this equation numerically to obtain the evolution of the wave shape and determine how the injected mass depends on the sample concentration in the reservoir. It is shown that due to the nonlinear coupling of the ionic concentrations and the electric field, the concentration of the injected sample could be substantially less than the concentration of the sample in the reservoir.

Keywords: electromigration dispersion; electrokinetic injection; nonlinear waves

1. Introduction

In microfluidic systems, electrokinetic injection is often employed in order to insert the sample from a reservoir into a microfluidic channel (Landers 1996; Camilleri 1998). A simplified problem, depicting the electrokinetic injection process, is shown in figure 1. The reservoir initially contains the sample dissolved in a background electrolyte of positive and negative ions. The channel contains only the background electrolyte. At time $t = 0$, a voltage, V , is applied to an electrode in the reservoir located far from the inlet, while the channel outlet (assumed infinitely far away) is electrically grounded. We describe how the concentration of the sample evolves with time as the sample moves into the micro-channel. For simplicity, we will assume that the capillary walls are uncharged, so that there is no electroosmotic flow.

When the concentration of sample in the reservoir is low, the dynamics is linear and is described by an advection–diffusion equation with constant advection speed. At high concentrations, the evolution is nonlinear owing to the phenomenon of electromigration dispersion. The physical mechanism of

*Author for correspondence (s-ghosal@northwestern.edu).

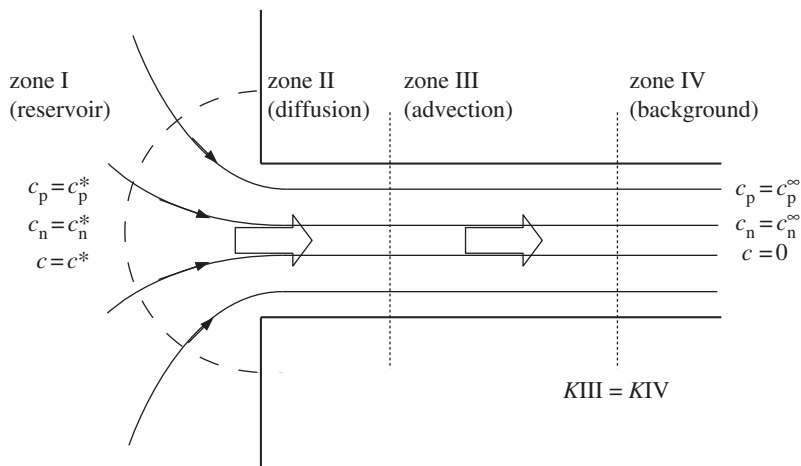


Figure 1. Schematic illustrating the electrokinetic injection of a sample (concentration c^* in the reservoir) into a micro-channel.

electromigration dispersion may be explained (Ghosal & Chen 2010*b*) in the following way: when the concentration of sample ions is significant in comparison with that of the background electrolyte, the electrical conductivity of the solution is locally altered. However, charge conservation and local electro neutrality require the electric current to be the same at all points along the axis of the capillary. Therefore, by Ohm's Law (ignoring, for the moment, the diffusive contributions to the current), the electric field must change axially, because, the product of the conductivity and electric field must remain constant. This varying electric field alters the effective migration speed of the sample ions, which, in turn, alters its concentration distribution. The transport problem for sample ions then becomes nonlinear and shock-like structures similar to those familiar from breaking water waves (Whitham 1974) can arise.

The problem has a certain similarity with the classical 'dam break problem' in hydrodynamics where a large stationary volume of water held back by a wall is suddenly released by partial or complete removal of the restraining wall (Ritter 1892; Stoker 1948; Whitham 1955). However, in the present problem, the driving mechanism is the variation of the electric field along the channel instead of hydrostatic pressure variations owing to changes in wave height.

In §2, we present the mathematical formulation for a minimal problem consisting of three ionic species: the analyte, a co-ion and a counter-ion, where the diffusivities of the three species are equal, the charge of the analyte is constant and the background electrolyte is fully dissociated. We will see that even in this highly idealized limit, the nonlinearities inherent in the system lead to surprising behaviour. The idealizations permit reduction of the problem to the solution of a single partial differential equation in one dimension. In §3, this equation is integrated numerically, and observations are presented for the behaviour of the sample ion concentration as it moves into the micro-channel. We find that at high concentrations, the concentration of sample ions that enter the micro-channel is significantly lower than that in the reservoir. In fact, as the concentration of sample ions in the reservoir is increased, the concentration within the injected

plug in the channel does not increase indefinitely but approaches a limiting value determined by the valence of the analyte ion and background electrolytes. In §4, we identify the reason for this behaviour and use simple arguments based on conservation laws to deduce the limiting value of the sample concentration in the channel. This is compared with results from the numerical simulations, and good agreement is found. Our findings are summarized in §5 and its implications in a broader context as well as its limitations are discussed.

2. Problem formulation

We consider a three-ion system consisting of sample ions, co-ions and counterions all of equal diffusivity (D). It follows, from the Einstein relation, that the mobility (u) of the three ionic species are also the same. However, the three species have different valences: z_p, z_n, z and therefore different electrophoretic mobilities: $\mu_p = z_p eu, \mu_n = z_n eu, \mu = z eu$, e being the proton charge. In this study, the suffix ‘p’ will generally indicate the positive ion (cation), ‘n’ will indicate the negative ion (anion) and the absence of a suffix will indicate the sample ion (analyte). Thus, z_p is positive, z_n is negative and z could be of either sign. The discussion in the rest of this section follows closely the earlier work of Ghosal & Chen (2010*b*).

We consider the simplest situation where the ions migrate from a semi-infinite reservoir to a uniform channel with no wall charge. Then, the problem is entirely one-dimensional, and the coupled equations describing the concentrations of the three ion species are

$$\frac{\partial c_p}{\partial t} + \frac{\partial}{\partial x}(z_p eu E c_p) = D \frac{\partial^2 c_p}{\partial x^2}, \quad (2.1)$$

$$\frac{\partial c_n}{\partial t} + \frac{\partial}{\partial x}(z_n eu E c_n) = D \frac{\partial^2 c_n}{\partial x^2} \quad (2.2)$$

and
$$\frac{\partial c}{\partial t} + \frac{\partial}{\partial x}(z eu E c) = D \frac{\partial^2 c}{\partial x^2}, \quad (2.3)$$

where E is the local electric field, x is the distance along the capillary and t is time. We will assume that the x -axis points in the direction of front motion from the reservoir into the capillary. As characteristic spatial scales are always much larger than the Debye length, local electro-neutrality holds (Ghosal & Chen 2010*a*). Thus,

$$z_p c_p + z_n c_n + z c = 0. \quad (2.4)$$

If we multiply equations (2.1)–(2.3) by the respective ionic charges, sum them and use equation (2.4), we get an equation that describes the constancy of electric current

$$\frac{\partial}{\partial x} [e^2 u (z_p^2 c_p + z_n^2 c_n + z^2 c) E] = 0. \quad (2.5)$$

Note that the net contribution from the diffusive fluxes vanishes exactly on account of the assumption of equal diffusivity of ions and local electro-neutrality.

Equation (2.5) may then be integrated to yield

$$(z_p^2 c_p + z_n^2 c_n + z^2 c)E = (z_p^2 c_p^\infty + z_n^2 c_n^\infty)E_\infty, \quad (2.6)$$

where E_∞ is the electric field in the capillary very far away from the inlet, and, c_n^∞, c_p^∞ are, respectively the corresponding negative and positive ion concentrations in the background electrolyte. Clearly, c_p^∞ and c_n^∞ are not independent but are related by the electro-neutrality condition

$$z_p c_p^\infty + z_n c_n^\infty = 0. \quad (2.7)$$

If we now introduce the Kohlrausch function (Kohlrausch 1897),

$$K(x, t) = \frac{(c_p + c_n + c)}{u}, \quad (2.8)$$

then it follows from equations (2.1)–(2.3) and (2.4) that K satisfies the diffusion equation

$$\frac{\partial K}{\partial t} = D \frac{\partial^2 K}{\partial x^2}. \quad (2.9)$$

The three algebraic relations: (2.4), (2.6) and (2.8) may be used to express all four dependent variables in the problem: c_p, c_n, c and E in terms of any one of them and the function $K(x, t)$. We choose to express all the variables in terms of c and K . These relations take a particularly simple form, if we use the normalized concentration

$$\phi = \frac{c}{c_n^\infty} \quad (2.10)$$

and

$$\theta(x, t) = \frac{uz_p}{z_p - z_n} \frac{K(x, t)}{c_n^\infty} \quad (2.11)$$

In terms of these variables, we then have

$$E = \frac{E_\infty}{\theta - \alpha\phi}, \quad (2.12)$$

$$\phi_p = \frac{c_p}{c_n^\infty} = -\frac{z - z_n}{z_p - z_n} \phi - \frac{z_n}{z_p} \theta \quad (2.13)$$

and

$$\phi_n = \frac{c_n}{c_n^\infty} = \frac{z - z_p}{z_p - z_n} \phi + \theta, \quad (2.14)$$

so that equation (2.3) gives the following evolution equation for ϕ :

$$\frac{\partial \phi}{\partial t} + \frac{\partial}{\partial x} \left(\frac{v\phi}{\theta - \alpha\phi} \right) = D \frac{\partial^2 \phi}{\partial x^2}, \quad (2.15)$$

where $v = zeuE_\infty$ is the velocity of an isolated sample ion in the constant electric field $E = E_\infty$, and following the notation of Ghosal & Chen (2010*b*), $\alpha = [(z - z_n)(z - z_p)]/z_n(z_p - z_n)$ is the ‘velocity–slope parameter’.

As θ is proportional to K , it is also a passive scalar. The initial and boundary conditions on θ in the domain $0 \leq x < \infty$ are

$$\theta(x, 0) = 1 \quad \text{if } x > 0, \quad (2.16)$$

$$\theta(0, t) = \theta^* \quad (2.17)$$

and

$$\theta(\infty, t) = 1, \quad (2.18)$$

where θ^* is the value of θ in the reservoir. The reservoir is considered to be ‘well mixed’, so that all ionic concentrations remain constant within it. An exact solution for θ may then be found using Fourier’s method,

$$\theta = \theta^* + (1 - \theta^*) \operatorname{erf} \left(\frac{x}{\sqrt{4Dt}} \right), \quad (2.19)$$

where

$$\operatorname{erf}(x) = \frac{2}{\sqrt{\pi}} \int_0^x e^{-y^2} dy \quad (2.20)$$

is the error function. Since the concentration of sample in the reservoir is being held constant at some value $\phi = \phi^*$, we have

$$\theta^* = \frac{c_n^*}{c_n^\infty} + \frac{z_p - z}{z_p - z_n} \phi^*. \quad (2.21)$$

The superscript $*$ indicates the value of the corresponding variable in the reservoir. Thus, c_n^* is the concentration of negative ions in the reservoir.

Equation (2.15), on the other hand, does not readily admit an analytical solution, because, unlike the equation for θ , it cannot be reduced to an ordinary differential equation by means of the similarity variable $\eta = x/\sqrt{4Dt}$. We will therefore obtain the time evolution of the normalized sample concentration $\phi(x, t)$ by substituting equation (2.19) in equation (2.15) and integrating the resulting one-dimensional partial differential equation numerically. Before we present this solution in §3, it is useful to note that at large distances from the reservoir, or more precisely, if $x \gg \sqrt{4Dt}$, equation (2.19) implies that $\theta \sim 1$, so that equation (2.15) reduces to

$$\frac{\partial \phi}{\partial t} + \frac{\partial}{\partial x} \left(\frac{v\phi}{1 - \alpha\phi} \right) = D \frac{\partial^2 \phi}{\partial x^2} \quad (2.22)$$

which was studied earlier by Ghosal & Chen (2010*b*).

3. Numerical simulations

We will find it convenient to express our results in terms of a characteristic length, w (the channel width), which gives a characteristic time w/v . Then clearly, the only parameters in the problem are $Pe = vw/D$, which may be regarded as a ‘Péclet number’ based on the electromigration speed, v , or a ‘field strength parameter’; the two valence ratios z_n/z , z_p/z ; and the parameter θ^* characterizing

the ionic composition of the mixture in the reservoir. For definiteness, we will assume that the sample is a cation ($z > 0$), and that

$$c_p^* = c_p^\infty. \quad (3.1)$$

This will be true, for example, if the electrolyte in the reservoir is prepared by adding the sample in solid form (so there is no dilution) to a stock solution of the background electrolyte that fills the micro-channel (because the sample contributes only counter-ions, the co-ion concentration is not altered). Using the electro-neutrality conditions,

$$\theta^* = 1 - \frac{z_p(z - z_n)}{z_n(z_p - z_n)}\phi^*. \quad (3.2)$$

The initial and boundary conditions for ϕ are

$$\phi(x, 0) = 0, \quad \text{if } x > 0 \quad (3.3)$$

$$\phi(0, t) = \phi^* \quad (3.4)$$

and

$$\phi(\infty, t) = 0. \quad (3.5)$$

We keep the valence ratios fixed at $z_p/z = 2$, $z_n/z = -1$.

Because we have reduced our problem to a one-dimensional one, the numerical integration is quite straightforward. We used a finite volume method to discretize equation (2.15) in space using an adaptive grid refinement algorithm that is enabled by applying the MATLAB library ‘MatMOL’ (Vande Wouwer *et al.* 2004). The spatially discretized system of equations is then integrated in time using the MATLAB solver ‘ode45’ (Shampine & Reichelt 1997) that is based on an explicit Runge–Kutta (4,5) formula.

Figure 2 shows the amount of sample that has moved into the reservoir at time t , defined as

$$m(t) = \frac{1}{w} \int_0^\infty \phi(x, t) dx. \quad (3.6)$$

Simulations are shown for $Pe = 10$ and 200. At long times, or more precisely, if $vt/w \gg Pe^{-1}$, the expected asymptotic form for $m(t)$ is

$$m(t) \sim \left(\frac{v\phi^*}{w} \right) t. \quad (3.7)$$

Figure 2 shows that indeed, at large times, $m(t) \propto t$. We determined the slope of the $m(t)$ curve at large times and plotted the dimensionless quantity $w\dot{m}/v$ as a function of ϕ^* in figure 3. It is seen that $w\dot{m}/v \sim \phi^*$ as long as $\phi^* \ll 1$ but as the concentration of sample in the reservoir is increased, the injection rate does not increase indefinitely but tends to saturate to a limiting value, that is, $w\dot{m}/v \sim \phi_m^* < \phi^*$.

The reason for this saturation of the injection rate may be understood by examining the concentration profiles $\phi(x, t)$ shown in figure 4. It is seen, that as the sample moves into the capillary, the concentration in the capillary is approximately equal to the concentration in the reservoir as long as this concentration remains small (figure 4a; $\phi^* = 0.01$). However, if the concentration in the reservoir is large (figure 4b; $\phi^* = 1$), then the concentration in the channel approaches a limiting value ϕ_m^* independent of the reservoir concentration.

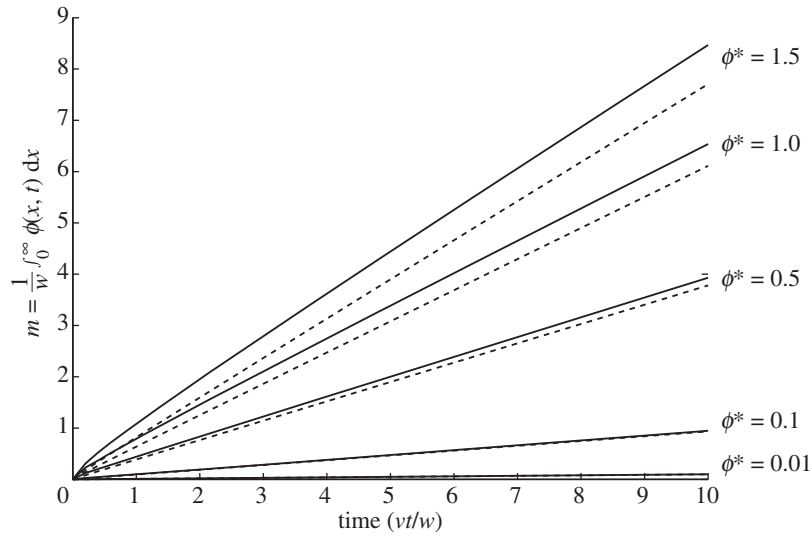


Figure 2. The increase of sample ions in the micro-channel as a function of dimensionless time at different dimensionless reservoir concentrations, ϕ^* . The solid line corresponds to $Pe = 10$ and the dashed line corresponds to $Pe = 200$.

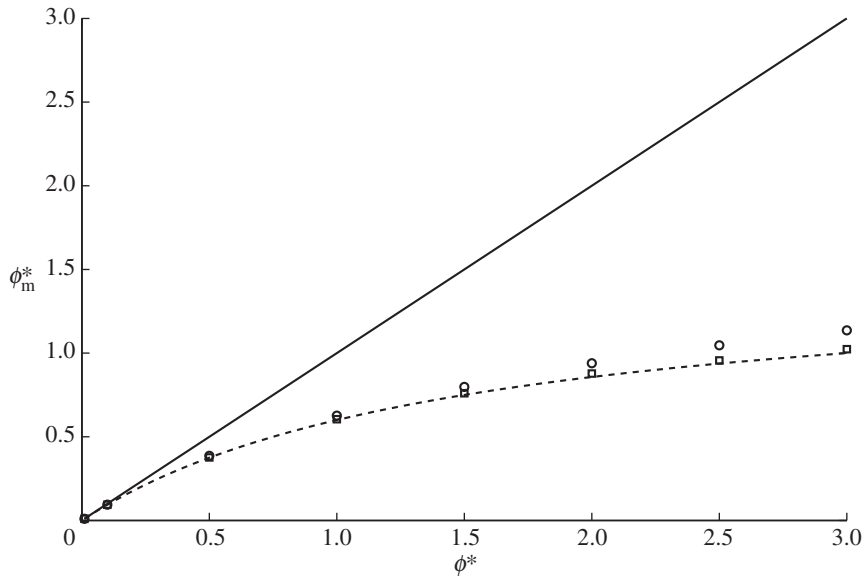


Figure 3. The normalized concentration of analyte in the micro-channel (ϕ_m^*) as a function of the corresponding quantity in the reservoir (ϕ^*). The solid line indicates the result expected from linear theory, the dashed line is the result predicted by the nonlinear theory, equation (4.7). The symbols (circle: $Pe = 10$; square: $Pe = 200$) are obtained by numerical integration of equation (2.15).

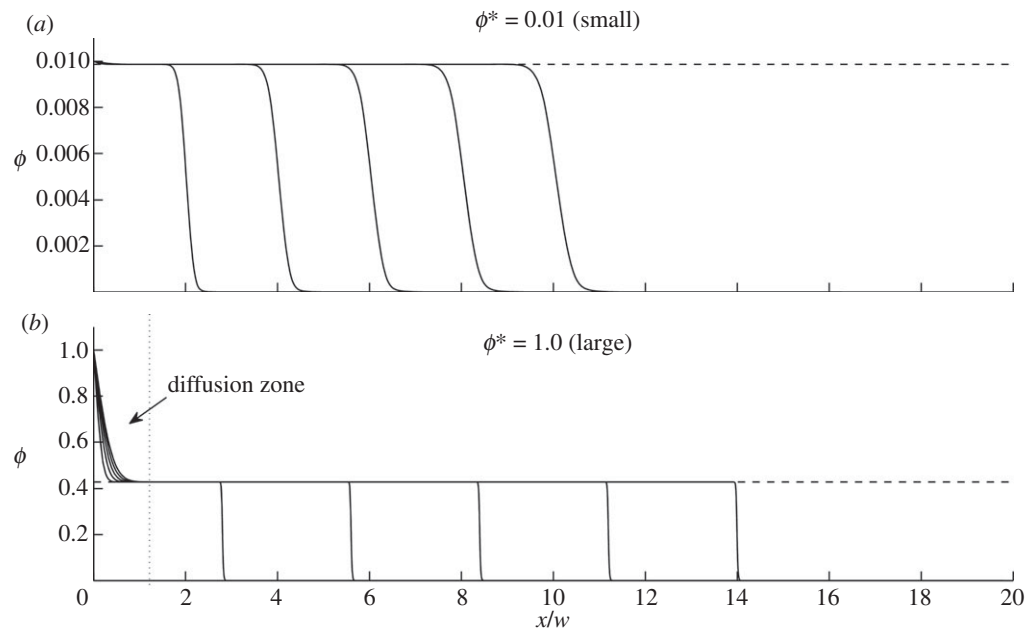


Figure 4. Concentration profiles in the micro-capillary at successive times: $vt/w = 2, 4, 6, 8, 10$. If the reservoir concentration is large (b), then a concentration jump develops at the entrance of the capillary, with a narrow diffusion zone connecting the values in the reservoir with the much smaller value of the concentration within the capillary. The concentration jump is insignificant if the reservoir concentration is small (a). The dashed line is ϕ_m^* evaluated using equation (4.8). Here $Pe = 200$.

In figure 5, we have reproduced the concentration distribution $\phi(x, t)$ that appears in figure 4b, together with the concentrations of the other ionic species $\phi_p(x, t)$ and $\phi_n(x, t)$, the local electric field $E(x, t)$, and, the local electrical conductivity owing to ions, $\sigma(x, t)$. These quantities are obtained from equations (2.12)–(2.14). The mechanism for the reduction of the concentration from $\phi = \phi^*$ in the reservoir to $\phi = \phi_m^* < \phi^*$ in the capillary may be understood from these graphs. At large values of the sample concentrations in the reservoir, there is a sharp rise in the solution conductivity in the immediate vicinity of the inlet resulting in a drop in the electric field. The flux of sample into the micro-channel is then determined by a combination of this greatly reduced electromigrational flux and the diffusive flux, and this is less than the expected flux indicated by equation (3.7) that should hold in the linear regime.

4. Analysis

An approximate theoretical determination of the critical concentration ϕ_m^* may be provided using the conservation equations. The method of doing this is in fact entirely analogous to that of the ‘moving boundary equations’ (Dole 1945) for describing advancing fronts (e.g. in isotachopheresis). The conceptual framework

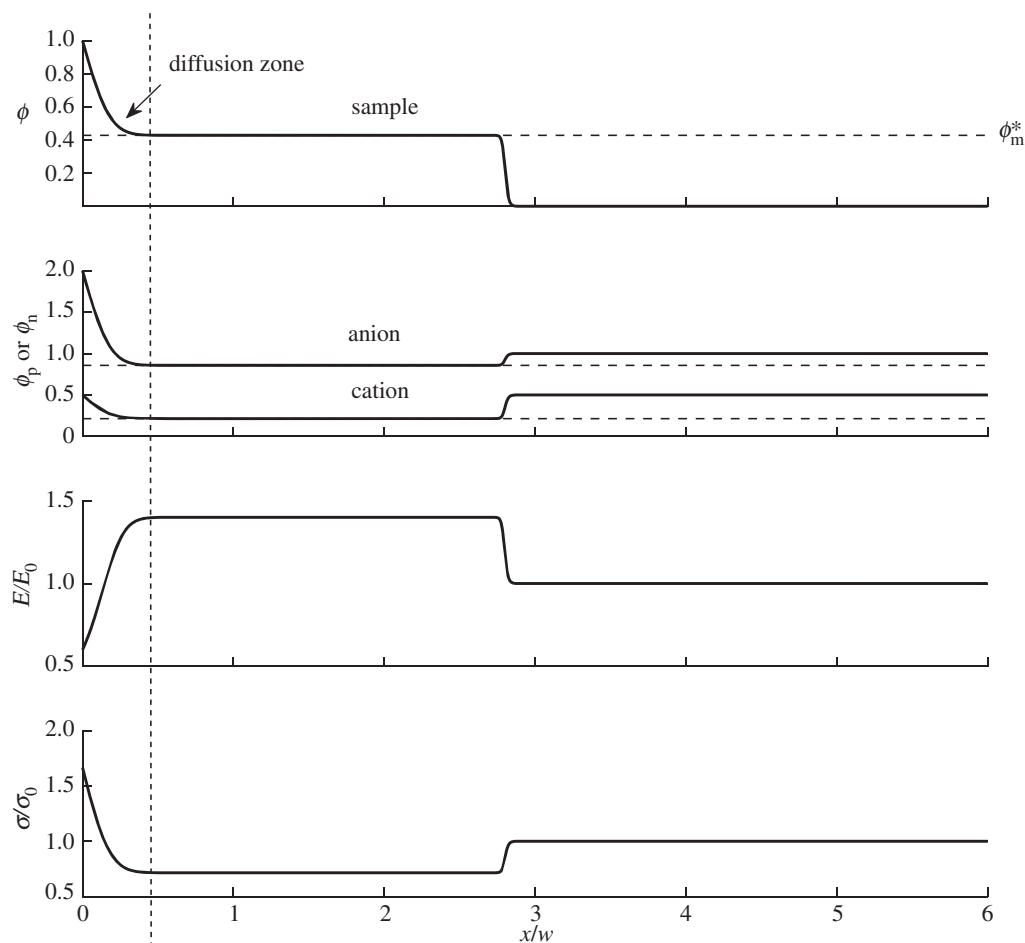


Figure 5. Same as in figure 4 except that profiles of all dependent variables are shown but at a fixed time instant, $vt/w = 2$. The dashed lines are the concentrations in the capillary calculated using equation (4.7). The bottom panel shows the electric conductivity (σ) normalized by its downstream value (σ_0).

is illustrated in figure 1. The domain is decomposed into four parts: (I) the ‘reservoir zone’ within the well mixed body of the reservoir where all concentrations are constant (II) the ‘diffusion zone’, which is the initial part of the micro-channel of length of order $\sqrt{2Dt}$ —here the ionic diffusive flux and the electromigrational flux driven by the electric field are comparable, (III) the ‘advection zone’ where diffusive fluxes are negligible (because concentration gradients are small) and ionic fluxes are primarily due to electromigration and (IV) the ‘background zone’ far downstream where the sample ions have not yet penetrated.

The boundary between the zones (I) and (II) is stationary (and located at the channel inlet) whereas the boundaries between the other zones propagate to the right. The arrows in figure 1 indicate fluxes of ions across the stationary

zone boundary. Equality of the fluxes for each species across the zone boundary require:

$$\pi r \phi^* E^{(I)}(r) = w E^{(III)} \phi_m^* \quad (4.1)$$

and

$$\pi r \phi_n^* E^{(I)}(r) = w E^{(III)} \phi_n^{(III)} \quad (4.2)$$

where $E^{(I)}(r)$ represents the electric field in the reservoir at a radial distance r from the inlet. The superscripts (I), (II), (III) or (IV) indicate the zone in which the corresponding variable is evaluated. Clearly, $\phi^{(I)} = \phi^*$, $\phi_n^{(I)} = \phi_n^*$ and $\phi^{(III)} = \phi_m^*$. Therefore, taking the ratio,

$$\phi_n^* = \left(\frac{\phi_n^{(III)}}{\phi_m^*} \right) \phi^*. \quad (4.3)$$

The Kohlrausch function, or, equivalently, $\theta(x, t)$, propagates only by diffusion. Therefore, $\theta(x, t)$ differs from unity only in zones (I) and (II). Thus,

$$\phi_n^{(III)} + \phi_p^{(III)} + \phi_m^* = 1 \quad (4.4)$$

The electro-neutrality condition (valid in all zones) for zone (III) is

$$z_p \phi_p^{(III)} + z_n \phi_n^{(III)} + z \phi_m^* = 0. \quad (4.5)$$

By combining equations (4.3) and (4.4) and using the electro-neutrality condition, equation (4.5), we get an equation for determining ϕ_m^*

$$\left(1 - \frac{z}{z_p} \right) \phi_m^* + r \left(1 - \frac{z_n}{z_p} \right) \phi_m^* = 1 - \frac{z_n}{z_p}, \quad (4.6)$$

where the ratio $\phi_n^*/\phi^* = r$ is a constant determined by the ionic composition of the electrolyte in the reservoir. Solving the equation (4.6) for ϕ_m^* , we have

$$\phi_m^* = \left[r + \frac{(z_p - z)}{(z_p - z_n)} \right]^{-1}. \quad (4.7)$$

In our numerical experiment, we assume that the sample is a cation, and that the co-ion concentration in the reservoir is the same as in the channel, so that $\phi_p^* = \phi_p^\infty = -z_n/z_p$. The electro-neutrality condition then implies that $\phi_n^* = 1 - (z/z_n)\phi^*$, so that equation (4.7) becomes

$$\phi_m^* = \frac{\phi^*}{1 + \xi \phi^*}, \quad (4.8)$$

where

$$\xi = -\frac{z_p(z - z_n)}{z_n(z_p - z_n)} \quad (4.9)$$

is a positive number. An expression for θ^* in terms of the sample ion concentration, ϕ^* , may also be derived by simple algebra:

$$\theta^* = 1 - \frac{z_p(z - z_n)}{z_n(z_p - z_n)} \phi^*. \quad (4.10)$$

In figure 3, we used equation (4.8) to plot ϕ_m^* as a function of ϕ^* . This curve is seen to describe very well the nonlinear saturation of the injected mass with increasing sample concentration in the reservoir.

The denominator in equation (2.15) vanishes, if $\phi = \theta/\alpha$. Far from the inlet, the singularity is approached as $\phi \rightarrow 1/\alpha$ (if $\alpha > 0$), because, $\theta \sim 1$. It was shown earlier (Ghosal & Chen 2010*b*) that the requirement of positivity of all ionic concentrations imposes a condition of self-consistency, $\phi(x, t) < \phi_c$ where

$$\phi_c = \begin{cases} \frac{(z_p - z_n)}{(z_p - z)}, & \text{if } z > 0 \\ -\frac{[z_n(z_p - z_n)]}{[z_p(z - z_n)]}, & \text{if } z < 0. \end{cases} \quad (4.11)$$

As, $\phi_c < 1/\alpha$, if $\alpha > 0$ (see appendix A), the singularity is never reached if initially ϕ is less than ϕ_c everywhere in the channel. This, however, leaves open the possibility that the initial condition $\phi(0, t)$ might be such that ϕ exceeds ϕ_c in some parts of the domain. We have now shown that if electrokinetic injection is used to insert the sample into the capillary, the shock at the inlet ensures that the injected sample concentration does not exceed $\phi_m^* < \phi_c$ (see appendix A), no matter how high the sample concentration in the reservoir may be. In capillary zone electrophoresis, one chooses the peak shape after electrokinetic sample injection as the ‘initial condition’. Then, the only initial conditions possible are the ‘realizable’ kind, where, $\phi(x, 0) < \phi_c$.

The speed of propagation of the analyte front in figure 4 may be readily calculated when the front is far from the inlet. To do this, we note that since $Pe = 200 \gg 1$ and $\theta \rightarrow 1$, equation (2.22) may be written as

$$\frac{\partial \phi}{\partial t} + \frac{\partial Q}{\partial x} = 0, \quad (4.12)$$

where

$$Q(\phi) = \frac{v\phi}{1 - \alpha\phi}. \quad (4.13)$$

Then, the shock propagation speed is given by (Whitham 1974) the Rankine-Hugoniot jump condition

$$V_s = \frac{Q(\phi_2) - Q(\phi_1)}{\phi_2 - \phi_1}, \quad (4.14)$$

where the subscripts 2 and 1 refer to conditions just behind the shock and just ahead of the shock, respectively. Putting $\phi_1 = 0$ and $\phi_2 = \phi_m^*$, we find, for the conditions shown in figure 4*b*, $\phi_m^* = 3/7 \approx 0.43$, so that $V_s = 1.405 v$. The shock speed determined from direct measurement of the front displacement in figure 4 is $1.4 v$, in close agreement with the theoretical prediction. In figure 4*a*, $\phi^* = 0.01$, so that $\phi_m^* \approx \phi^*$. In this case, both the theoretical and the measured values give $V_s \approx v$.

5. Conclusions

The problem of electromigration of a sample ion from a large reservoir into a confined channel in the presence of a fully dissociated background electrolyte was studied in the idealized situation where all ionic species have the same diffusivity. If the sample ion concentration is small compared with that of the background electrolyte, the behaviour of the system is exactly as one might expect. When the electric field is switched on, a sample plug with concentration equal to that in the reservoir, is drawn into the microchannel. However, if the sample ion concentration is comparable or large compared with the background electrolyte, then the behaviour of the system is dominated by the intrinsic nonlinearity of the electro-diffusional problem, and the outcome is quite counterintuitive. Once again, the sample is drawn into the microchannel as a plug of increasing length, but the concentration of sample ions in the plug is less than in the reservoir. In fact, as the reservoir concentration is progressively increased, the concentration of sample ions in the capillary approaches a limit that depends on the valences of the three ionic species but is independent of the reservoir concentration.

In an earlier paper (Ghosal & Chen 2010*b*), the authors presented a theory of electromigration of a sample in an infinitely long micro-channel when only three ions of equal diffusivity are present. There, it was shown that the requirement that none of the three ionic concentrations could ever be negative, put a limit to the validity of the theory. It was therefore required that the initial condition be such that the dimensionless sample concentration not exceed a certain (positive) critical concentration, ϕ_c . Here, we have shown that initial conditions that do not satisfy this requirement cannot arise if the analyte is introduced into the micro-capillary by electrokinetic injection. In fact, the diffusional boundary layer at the channel entrance ensures that the concentration of analyte drawn into the micro-capillary is always less than ϕ_c . Thus, the critical concentration can never be exceeded if the sample is introduced by electrokinetic injection, and consequently, the singularity at $\phi = 1/\alpha$ (if $\alpha > 0$), inherent in equation (2.22) is never reached.

One may question whether the strongly nonlinear regime considered here is of relevance to actual laboratory practice. The answer depends on the numerical value of the critical concentrations, ϕ_m^* and ϕ_c . If the sample and carrier ions have similar valences, then these critical concentrations are all of order unity. Thus, to approach these critical values, the sample ions in the injected plug will need to be present at concentrations approaching that of the carrier electrolyte. Such high concentrations are normally not employed in laboratory practice with capillary electrophoresis. However, if the sample is a macro-ion, then the critical values may actually be quite small. For example, at pH 2.0 Bovine serum albumin has a valence, $z \sim 55$ (Ford & Winzor 1982). Then, in a univalent carrier electrolyte, we have $\phi_c \sim 0.04$, so that the strongly nonlinear regime studied here may be easily reached.

The shock-like transition in concentration at the entrance of the micro-channel observed here is reminiscent of ‘desalination shocks’ that propagate outward from micro-channel/nano-channel junctions (Mani *et al.* 2009; Zangle *et al.* 2009) or from the surface of a perm-selective membrane embedded in a microfluidic channel. The mechanism of these shocks is related to the nonlinear coupling between the ion-depletion zone (owing to concentration polarization) near the membrane with the electric Debye layers at the walls of the micro-channel.

The problem considered here is much simpler; Debye layers or concentration polarization is not involved. Nevertheless, it is another example of shock-like behaviour that may be traced to the nonlinear nature of the underlying Nernst–Planck–Poisson system of equations for ionic transport. As in the case of desalination shocks, the effect described here would also be relevant for solutes electromigrating into porous media (Mani & Bazant 2011) or electromigration of analytes through variable geometry channels, such as pores in membranes, where lubrication theory (Ghosal 2002) can be used to generalize the analysis presented here. Finally, if the channel walls are charged, then electroosmotic flow would arise, so that the transport problem becomes intrinsically two- or three-dimensional. In such cases, homogenization can be used to achieve a reduced description, as shown by Ghosal & Chen (2012) for electromigration in an infinitely long uniform channel.

Support from the National Institute of Health (NIH) under grant no. R01EB007596 is gratefully acknowledged.

Appendix A. Proof of the inequality $\phi_m^* < \phi_c < 1/\alpha$

If $\alpha > 0$, $z_p > z > z_n$. Then

$$\alpha\phi_c = \begin{cases} \frac{z_p - z_n}{z_p - z} \frac{(z - z_n)(z - z_p)}{z_n(z_p - z_n)} = \frac{-z_n + z}{-z_n} < 1, & \text{if } z < 0 \\ -\frac{z_n}{z_p} \cdot \frac{z_p - z_n}{z - z_n} \frac{(z - z_n)(z - z_p)}{z_n(z_p - z_n)} = \frac{z_p - z}{z_p} < 1, & \text{if } z > 0 \end{cases} \quad (\text{A } 1)$$

thus, $\phi_c < 1/\alpha$ if $\alpha > 0$.

To prove the first part of the inequality, $\phi_m^* < \phi_c$, we first show that $r > -z/z_n$. This is clearly true if $z < 0$. To show this when $z > 0$, first we use the electro-neutrality condition to express ϕ_p^* in terms of the other variables:

$$\phi_p^* = -\frac{z}{z_p}\phi^* - \frac{z_n}{z_p}\phi_n^* = \frac{\phi^*}{z_p}(-z - rz_n). \quad (\text{A } 2)$$

Now, we must have $\phi_p^* > 0$. This is always true if $z < 0$, but if $z > 0$, we require that $r > -z/z_n$.

We will now show that $\phi_m^* < \phi_c$ by considering the two cases $z > 0$ and $z < 0$ separately. First suppose that $z < 0$. Then

$$\phi_m^* = \frac{1}{r + (z_p - z)/(z_p - z_n)} < \frac{1}{(z_p - z)/(z_p - z_n)} = \frac{z_p - z_n}{z_p - z} = \phi_c. \quad (\text{A } 3)$$

Now suppose that $z > 0$. Then

$$\phi_m^* = \frac{1}{r + (z_p - z)/(z_p - z_n)} \quad (\text{A } 4)$$

$$< \frac{1}{-(z/z_n) + (z_p - z)/(z_p - z_n)} = -\frac{z_n}{z_p} \frac{z_p - z_n}{z - z_n} = \phi_c. \quad (\text{A } 5)$$

Thus, in all cases, $\phi_m^* < \phi_c$ which completes the proof.

References

- Camilleri, P. (ed.) 1998 *Capillary electrophoresis, theory and practice*. Boca Raton, FL: CRC Press.
- Dole, V. P. 1945 A theory of moving boundary systems formed by strong electrolytes. *J. Am. Chem. Soc.* **67**, 1119–1126. (doi:10.1021/ja01223a025)
- Ford, C. L. & Winzor, D. J. 1982 Measurement of the net charge (valence) of a protein. *Biochim. Biophys. Acta* **703**, 109–112. (doi:16/0167-4838(82)90017-6)
- Ghosal, S. 2002 Lubrication theory for electroosmotic flow in a microfluidic channel of slowly varying cross-section and wall charge. *J. Fluid Mech.* **459**, 103–128. (doi:10.1017/S0022112002007899)
- Ghosal, S. & Chen, Z. 2010a A nonlinear equation for ionic diffusion in a strong binary electrolyte. *Proc. R. Soc. A* **466**, 2145–2154. (doi:10.1098/rspa.2010.0028)
- Ghosal, S. & Chen, Z. 2010b Nonlinear waves in capillary electrophoresis. *Bull. Math. Biol.* **72**, 2047–2066. (doi:10.1007/s11538-010-9527-2)
- Ghosal, S. & Chen, Z. 2012 Electromigration dispersion in a capillary in the presence of electroosmotic flow. *J. Fluid Mech.* **697**, 436–454. (doi:10.1017/jfm.2012.76)
- Kohlrausch, F. 1897 Ueber concentrations-verschiebungen durch electrolyse im inneren von lösungen und lösungsgemischen. *Ann. Phys.* **62**, 209–239. (doi:10.1002/andp.18972981002)
- Landers, J. (ed.) 1996 *Introduction to capillary electrophoresis*. Boca Raton, FL: CRC Press.
- Mani, A. & Bazant, M. Z. 2011 Deionization shocks in microstructures. *Phys. Rev. E* **84**, 061504. (doi:10.1103/PhysRevE.84.061504)
- Mani, A., Zangle, T. A. & Santiago, J. G. 2009 On the propagation of concentration polarization from microchannel–nanochannel interfaces Part I: analytical model and characteristic analysis. *Langmuir* **25**, 3898–3908. (doi:10.1021/la803317p)
- Ritter, A. 1892 Die fortpflanzung der wasserwellen. *Ver. Deutsch ingenieur zeitschr* **36**, 947–954.
- Shampine, L. F. & Reichelt, M. W. 1997 The MATLAB ODE suite. *SIAM J. Sci. Comput.* **18**, 1. (doi:10.1137/S1064827594276424)
- Stoker, J. 1948 The formation of breakers and bores the theory of nonlinear wave propagation in shallow water and open channels. *Commun. Appl. Math.* **1**, 1–87. (doi:10.1002/cpa.3160010101)
- Vande Wouwer, A., Saucez, P. & Schiesser, W. E. 2004 Simulation of distributed parameter systems using a Matlab-based method of lines toolbox: chemical engineering applications. *Ind. Eng. Chem. Res.* **43**, 3469–3477. (doi:10.1021/ie0302894)
- Whitham, G. B. 1955 The effects of hydraulic resistance in the dam-break problem. *Proc. R. Soc. Lond. A* **227**, 399–407. (doi:10.1098/rspa.1955.0019)
- Whitham, G. 1974 *Linear and nonlinear waves*. New York, NY: Wiley-Interscience.
- Zangle, T. A., Mani, A. & Santiago, J. G. 2009 On the propagation of concentration polarization from microchannel–nanochannel interfaces part II: numerical and experimental study *Langmuir* **25**, 3909–3916. (doi:10.1021/la803318e)